Measurement-Induced Dark State Phase Transitions in Long-Ranged Fermion Systems

T. Müller, S. Diehl, and M. Buchhold
Institut für Theoretische Physik, Universität zu Köln, D-50937 Cologne, Germany

We identify an unconventional algebraic scaling phase in the quantum dynamics of long-range hopping, free fermions, which are exposed to continuous local measurements. The algebraic phase occurs for hopping decay exponents $1 < p \lesssim 3/2$, and features an algebraic entanglement entropy growth, and a slow algebraic decay of the density-density correlation function, both with a fractional exponent. It is separated from a critical phase with logarithmic entanglement growth at small, and an area law phase with constant entanglement entropy at large monitoring rates. A perturbative renormalization group analysis predicts that the transitions to the long-range phase correspond to an unconventional, modified sine-Gordon theory. Exact numerical simulations of the monitored wave functions are in excellent agreement with an analytical replica field theory approach, which confirms the view of the measurement-induced phase transition as a quantum phase transition in the dark state of an effective, non-Hermitian Hamiltonian.

Augmenting the unitary quantum evolution with projective or continuous measurements advances the phenomenology of nonequilibrium quantum systems and provides a new angle for understanding quantum dynamics [1–25]. One particular scenario are measurement-induced phase transitions (MIPT), which arise in wave functions that evolve under the interplay of unitary time evolution and frequent local measurements, and where the measurement outcomes are tracked along each trajectory [1–17]. Because of the Hermiticity of measurement operators, the averaged quantum dynamics, corresponding to unread measurements, follows a Lindblad master equation with Hermitian jump operators, which converges towards a featureless infinite temperature state [26–29]. The extensive configurational entropy generated by all possible measurement outcomes erases all the information on individual trajectory wave functions. However, individual wave functions preserve nontrivial quantum features, and can undergo a MIPT, which is witnessed by state dependent, nonlinear observables, e.g., the entanglement entropy or connected correlation functions.

So far, two major types of MIPTs have been identified by their entanglement growth with system size L. One is represented by transitions from a volume ($S \sim L$) to an area law ($S \sim L^0$) [1–9], and observed for random circuits and certain interacting Hamiltonians [10–12]. A second type are transitions from a critical phase with a logarithmic growth of entanglement entropy ($S \sim \log L$), again to an area law [13–17].

This calls for the question, whether this is the exhaustive set of phases and phase transitions that can exist in monitored quantum dynamics. Promising candidates for exploring it are systems with long-ranged generators of dynamics: Long-ranged Hamiltonians are known to induce new phases in ground states, and to qualitatively modify the critical behavior at phase transitions [30–32]. The thus achieved redistribution of particles over large distances strongly modifies the entanglement dynamics and the spreading of correlations [33–35]. Experimental platforms for engineering such Hamiltonians range from trapped ions [35–38], cold atoms in cavities [39,40], Rydberg atoms [41], and polar molecules [42].

In this work, we explore an elementary model of monitored, long-ranged dynamics: Free fermions with variably ranged hopping, characterized by an algebraic range exponent p [see Fig. 1(a)], competing with disentangling, local particle number measurements. As a main result, we demonstrate that the long-range entangling evolution leads to the emergence of an unconventional dynamical phase, in which the entanglement entropy grows with the system size $S \sim L^b$ with $b = 3/2 - p$ [43], faster than logarithmically but slower than the volume law of fully ergodic dynamics [44]. Furthermore, the phase features nonlinear density-density correlation functions, which follow an algebraic decay $\sim L^{-a}$ with $a = p + 1/2$. This phase is realized for exponents $1 < p < p_c = 3/2$, irrespective of the strength of measurement $\gamma > 0$: Local measurements cannot supersede the entanglement generated by long-range coherent hopping. This implies the existence of a tricritical point, where a conformally invariant phase with logarithmic entanglement growth, an area law phase, and the long-range phase meet [see Figs. 1(b), 1(c)].

To establish these results, we employ a combination of numerical simulations [13,16,45] and an analytical replica field theory [14], in which the steady state under monitoring emerges as the dark state of an effective, non-Hermitian sine-Gordon Hamiltonian. The measurements then favor
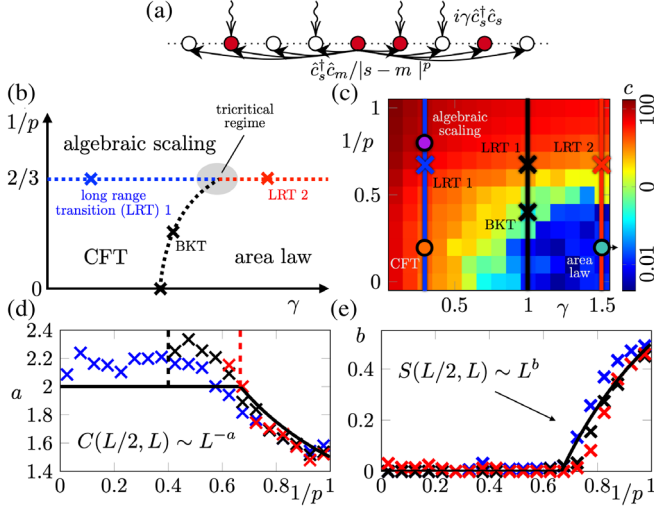
FIG. 1. (a) Free fermions on a chain with algebraic hopping $(1 < p < \infty)$ and continuous monitoring with rate γ. (b) Schematic phase diagram: we detect and characterize three qualitatively different phases. (c) Phase diagram as determined from the effective central charge c for $L = 600$. Circles indicate the points discussed in Fig. 2. The color-coded vertical lines are studied in (d),(e): comparison of the numerically determined scaling exponents at $\gamma = 0.3$ (blue), $\gamma = 1$ (black) and $\gamma = 1.5$ (red) with the dark state (solid black line). (d) Correlation function exponent a. Dashed lines yield an estimate for the point where the algebraic scaling terminates and is replaced by exponential scaling. (e) Entanglement entropy growth exponent b. A vanishing exponent corresponds to logarithmic scaling or area law. The critical points found by this procedure are indicated as crosses in (c).

the evolution into an eigenstate of the measurement operators, i.e., a state with a fixed particle number $n_l = 0, 1$ at each site. In the Hamiltonian framework, this corresponds to a pinning of the density fluctuations [14]. This mechanism competes with the long-range hopping, which establishes long-range coherent states, corresponding to a pinning of the conjugate phase. The analytical results align well with the numerical simulations, predicting the critical value of p and the scaling exponents in the long-range phase with high accuracy.

Microscopic model and effective Hamiltonian.—We consider fermions on a ring of L sites (labeled s, m), which are created and annihilated by the operators, $\hat{c}_s^\dagger, \hat{c}_s$ with $\{\hat{c}_s, \hat{c}_m^\dagger\} = \delta_{s,m}$, $\hat{n}_s = \hat{c}_s^\dagger \hat{c}_s$. The long-range hopping Hamiltonian is

$$\hat{H} = -\sum_{s \neq m} t_{s,m} \hat{c}_s^\dagger \hat{c}_m, \qquad t_{s,m} = |s - m|^{-p}. \qquad (1)$$

Its range is set by the exponent p and decreases with larger p, reproducing nearest-neighbor hopping for $p \to \infty$ [13,14,45]. We consider $p > 1$, ensuring a well-defined thermodynamic limit with a non-singular fermion dispersion.

In order to implement measurement of the wave function, we consider a standard continuous measurement protocol, known as quantum state diffusion [46,47]. It yields the stochastic Schrödinger equation (SSE),

$$d|\psi\{\xi_{s,t}\}\rangle = \left[-i\hat{H}dt + \sum_s \left(\xi_{s,t}\hat{M}_{s,t} - \frac{\gamma}{2}\hat{M}_{s,t}^2 dt \right) \right] |\psi\{\xi_{s,t}\}\rangle. \qquad (2)$$

Here, γ is the dimensionless monitoring strength, $\hat{M}_{s,t} = \hat{n}_s - \langle\psi\{\xi_{s,t}\}|\hat{n}_s|\psi\{\xi_{s,t}\}\rangle$ are the *monitoring operators* and $\xi_{s,t}$ is a Gaussian white noise with zero mean $\overline{\xi_{s,t}} = 0$ and short-ranged correlations $\overline{\xi_{s,t}\xi_{m,t'}} = \gamma dt \delta_{s,m}\delta(t - t')$. The overbar denotes the noise or trajectory average. The SSE is realized by coupling the local observable $\hat{n}_s$ to a continuum of bath degrees of freedom, e.g., pointers [47,48], which is read out continuously, e.g., via homodyne detection [49]. Equation (2) is quadratic in $\hat{c}_s, \hat{c}_s^\dagger$ and number conserving, and can be efficiently simulated with Gaussian wave functions. We start from the half-filled Néel state, and evolve the system until a stationary state is reached.

The random measurement outcomes generate a large configurational entropy: each allowed measurement outcome appears with equal probability in the long-time limit. This is reflected in the conditioned density matrix $\rho_{c,t} \equiv |\psi\{\xi\}\rangle\langle\psi\{\xi\}|$, whose trajectory average always yields a maximally mixed state $\overline{\rho_{c,t}} \sim \mathbb{1}$. The nontrivial quantum dynamics of individual wave functions $|\psi\{\xi\}\rangle$, however, is encoded in nonlinear trajectory averages of $\rho_{c,t}$ [9,14,50,51]. Examples are the entanglement entropy or conditioned correlation functions.

In order to access nonlinear observables analytically, we apply the *replica field theory* for MIPTs put forward in Ref. [14]. It introduces the product of two *replicated* density matrices $\rho_{c,t} \otimes \rho_{c,t}$, which allows us to separate the measurement randomness (accumulating it in an effective center-of-mass coordinate) from the inherent quantum evolution of the wave functions [14]. For fermions in one spatial dimension, the latter becomes particularly accessible due to bosonization. The quantum degrees of freedom are then mapped onto boson field operators $\hat{\phi}_x, \hat{\theta}_x$, obeying the canonical commutation relation $[\hat{\phi}_y, \partial_x\hat{\theta}_x] = i\delta(x - y)$. Here we extend the replica field theory to long-range hopping fermions. The steady state $|\psi_D\rangle$ of the SSE (2) then is equivalent to the *dark state* of an effective, non-Hermitian Hamiltonian, i.e.,

$$\hat{H}_{\text{eff}}|\psi_D\rangle = 0, \quad \text{with} \quad \hat{H}_{\text{eff}} = \hat{H}_{\text{sr}} + \hat{H}_{\text{lr}}. \qquad (3)$$

The Hamiltonian consists of a short-ranged part $\hat{H}_{\text{sr}}$ and a long-ranged part $\hat{H}_{\text{lr}}$ with (see Ref. [52] for a derivation)

$$\hat{H}_{\rm sr} = \int_x \{\eta^{-1}(\partial_x\hat{\theta}_x)^2 + \eta(\partial_x\hat{\phi}_x)^2 - i\lambda[1-\cos\sqrt{8}\hat{\phi}_x]\}, \quad (4a)$$

$$\hat{H}_{\rm lr} = i\Delta \int_{x,|y|>1} |y|^{-2p}\{1 + \cos[\sqrt{2}(\hat{\theta}_x - \hat{\theta}_{x+y})]\}. \quad (4b)$$

$\hat{H}_{\rm sr}$ covers both the nearest neighbor hopping and the measurements of the local particle density. It is of the sine-Gordon form with $\eta^2 = 1 - (2\gamma i/\pi)$ and $\lambda > 0$, and has been derived in Ref. [14]. $\hat{H}_{lr}$ contains hoppings across more than one site $\hat{c}_l^\dagger\hat{c}_{l+m} \sim e^{i(\hat{\theta}_l - \hat{\theta}_{l+m})}$, $m > 1$ to leading order in bosonization $\hat{c}_l^\dagger\hat{c}_{l+m}$ (see Ref. [52] for details).

The effective Hamiltonian has two remarkable features, which emerge from the replica theory and leave clear signatures in the fermion observables: First, due to the monitoring $\hat{H}_{\rm lr}$ is purely imaginary ($\Delta > 0$), although the original fermion hopping is Hermitian. Second, the effective hopping amplitude decays with an exponent $\sim 2p$, which is twice as large as for the microscopic amplitude.

Observables.—We characterize the steady state of the SSE (2), in terms of trajectory averages of the von-Neumann entanglement entropy S and of the connected density-density correlation function C for fixed system size L,

$$S(l, L) = \overline{-\text{Tr}\rho_l \log\rho_l}, \quad (5a)$$

$$C(l, L) = \overline{\langle\hat{n}_x\hat{n}_{x+l}\rangle - \langle\hat{n}_x\rangle\langle\hat{n}_{x+l}\rangle} = \overline{|\langle\hat{c}_x^\dagger\hat{c}_{x+l}\rangle|^2}. \quad (5b)$$

Here, $\rho_l = \text{Tr}_{L\backslash l}|\psi\{\xi\}\rangle\langle\psi\{\xi\}|$ is the reduced density matrix of a subsystem of length l and the expectation value is taken with respect to the numerically simulated steady state $|\psi\{\xi\}\rangle$.

Remarkably, both of these quantities can be analytically calculated within the replica field theory (where $L \to \infty$). Their leading behavior is captured by a simple form [52],

$$S(l) = \frac{1}{3}\langle\hat{\phi}_x\hat{\phi}_{x+l}\rangle, \qquad C(l) = \frac{1}{2\pi^2}\partial_l^2\langle\hat{\phi}_x\hat{\phi}_{x+l}\rangle. \quad (6)$$

Here the expectation value is taken with respect to the dark state $|\psi_D\rangle$. The form of $C(l)$ follows from $\hat{n}_x \to \rho_0 - (\partial_x\hat{\phi}_x/\pi)$, and the entropy formula is obtained under the assumption of free Dirac fermions in Gaussian states [14,15,55–57].

Dark state phase structure.—Based on the properties of the steady state wave function, we qualitatively distinguish three phases [see Fig. 1(b)]: (i) An area law phase for large monitoring ($\gamma \gtrsim 1$) and short-ranged hopping ($p > 3/2$), (ii) a conformally invariant (CFT) phase for small but nonvanishing monitoring and short-ranged hopping ($p > 3/2$), and (iii) a novel algebraic scaling phase due to long-range hopping ($p < 3/2$). We show representative results for each phase in Fig. 2. Additionally, isolated at $\gamma = 0$, a volume law is realized, crossing over to small system sizes for $\gamma > 0$ [13].
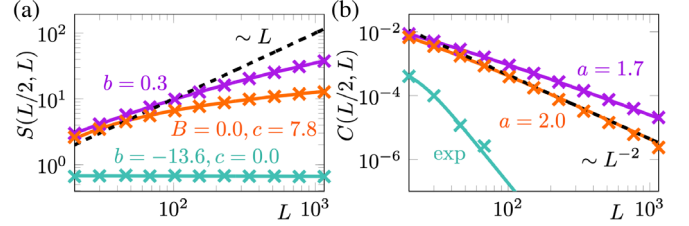

FIG. 2. Phase characterization of conformally invariant ($\gamma = 0.3$, $p = 1.25$, orange), area-law ($\gamma = 2$, $p = 5$, light blue), and algebraic scaling phase ($\gamma = 0.3$, $p = 5$, purple). (a) Half-system entanglement entropy and best fit using the ansatz $S = (c/3)\log(L/\pi) + s_0 + BL^b$. The entropy always grows slower than a volume law ($\sim L$, dashed line). (b) The scaling exponent of the correlation function at opposite ends of the system is determined by fitting to $C = 1/[AL^a + DL]$ (dashed line $\sim L^{-2}$).

Numerically, we combine two approaches to distinguish the three phases, and their boundaries. (1) Informed by logarithmic growth of the entanglement entropy in the CFT phase, $S(L/2, L) \sim (c/3)\log(L)$, we assume a logarithmic scaling of $S(L/2, L)$ and extract a size-dependent prefactor $c(L)$. In the area-law phase and in the CFT phase, $c(L)$ saturates as a function of the system size. In the algebraic phase it does not saturate, indicating faster than logarithmic growth of $S(l, L)$ on large distances [see Fig. 1(c), Fig. 3(a)], allowing us to localize the phase boundaries. (2) We make a general ansatz for $S(L/2, L)$ and $C(L/2, L)$, including both algebraic and logarithmic scaling and compute the best fit as a function of L (see Fig. 2). For sufficiently large system sizes (up to $L = 2048$), the fits then converge to *either* a logarithmic *or* an algebraic form. This yields consistent results for the scaling behavior in each regime, as well as for the scaling exponents and the location of the phase boundaries [see Figs. 1(d), 1(e)]. We further confirm these results by a third approach (see Ref. [52]), where we vary the subsystem size l.
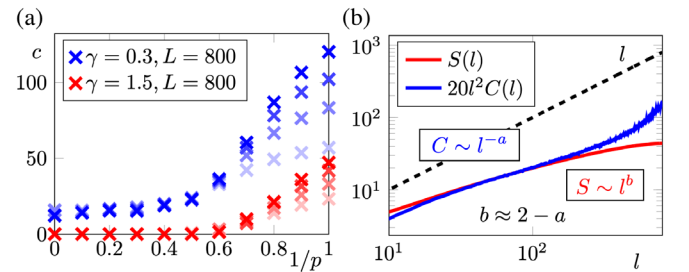

FIG. 3. (a) Effective central charge c determined from a fit at $l \in [L/4, 3L/4]$ for system sizes $L = 200, 400, 600, 800$. For $1/p \lesssim 0.6$, c saturates, while it diverges with L for $1 > 1/p \gtrsim 0.6$, indicating faster than log entanglement growth. (b) Entanglement entropy and density-density correlation function deep in the algebraic scaling phase ($\gamma = 0.3$, $p = 1.25$) for $L = 1600$. At intermediate distances, where finite-size effects are negligible, the algebraic scaling matches the analytical prediction $b = 2 - a$.

The three distinct, numerically observed phases are predicted also analytically from the structure of H_{eff}. The Hamiltonian consists of a free part, quadratic in $\hat{\theta}_x, \hat{\phi}_x$, and two competing nonlinearities, $\cos\sqrt{8}\hat{\phi}_x$, $\cos[\sqrt{2}(\hat{\theta}_x - \hat{\theta}_y)]$. The structure of the dark state $|\psi_D\rangle$ depends on whether or not those nonlinearities are relevant on large distances. Both of them tend to suppress fluctuations and to pin the fields in their argument to a fixed value. However, $\hat{\theta}_x, \hat{\phi}_x$ are conjugate and cannot be pinned simultaneously. Therefore at most one nonlinearity can be relevant. This gives rise to the three scenarios outlined above: (i) in the area law phase, $\cos\sqrt{8}\hat{\phi}_x$ is relevant and pins the density field $\hat{\phi}_x$ to a measurement eigenstate, $\hat{\phi}_x|\psi_D\rangle = \Phi_x|\psi_D\rangle$ with $\Phi_x \in \mathbb{R}$. (ii) in the CFT phase, neither of the cosine terms are relevant and both can be dropped. This yields a scale invariant free boson Hamiltonian. (iii) in the algebraic scaling phase, the long-range hopping $\cos[\sqrt{2}(\hat{\theta}_x - \hat{\theta}_y)]$ is relevant and yields a pinning of the relative phases $\hat{\theta}_x - \hat{\theta}_{x+l}$ of the fermions. This yields long-range correlations in $\hat{\theta}_x$ and increased local density fluctuations $\sim\hat{\phi}_x$.

The regimes (i) and (ii) are established for the limit $p \to \infty$ (numerically in Refs. [13,15] and analytically in Ref. [14]). In the following, we thus focus on the new algebraic regime (iii) and the phase transitions (i)↔(iii) and (ii)↔(iii). Canonical power counting of the cosine vertex yields the scaling dimension $[\Delta] = 3 - 2p$ [58]. It shows that the long-range aspect of the hopping is irrelevant for $p > 3/2$, and explains why the algebraic phase is located at $p < 3/2$. The numerical simulations confirm the independence of the critical value $p_c = 3/2$ from the measurement strength $\gamma > 0$, shown in Figs. 1(d), 1(e). This implies that even frequent local measurements cannot overcome the entanglement generation of a long-ranged kinetic Hamiltonian, which we confirm analytically below.

Characterizing the phase transitions.—The three different phases discussed above are separated from each other by three different types of phase transitions (illustrated in Fig. 1). Each phase transition features a characteristic competition between different parts of the effective Hamiltonian: the quadratic part ($\sim\eta, \eta^{-1}$) tends to balance the fluctuations of $\hat{\phi}_x, \hat{\theta}_x$, while the nonlinearities ($\sim\Delta, \lambda$) suppress fluctuations of $\hat{\theta}_x$ or $\hat{\phi}_x$. In order to reveal and analyze this competition, we investigate the perturbative renormalization group (RG) equations for η, Δ, λ.

The RG equations are obtained by rescaling spacetime with a factor $b = e^{-s}$, i.e., $dx, dt \to bdx, bdt$, with s infinitesimal, and then integrating out fast modes with momentum $b\Lambda < |q| < \Lambda$ (with short distance cutoff $\Lambda = \pi$). The first order RG equations are (see Ref. [52])

$$\partial_s\Delta = (3 - 2p - \eta)\Delta, \qquad (7)$$

$$\partial_s\eta = -\eta^2\Delta. \qquad (8)$$

Similar equations have been obtained in Ref. [32] for the ground state of a Hermitian, long-range interacting *XXZ* chain. Here, however, all couplings are complex, and the canonical scaling dimension of the long-range coupling Δ is modified compared to the Hermitian case [32] by replacing $p \to 2p$. The quantum phase transitions observed here thus represent a generalization of ground state phase transitions in unitary systems, to dark state MIPTs.

The RG equations (7), (8) yield several insights: (a) For $p > 3/2$, the long-range hopping $\sim\Delta$ is always irrelevant and any initial $\Delta \neq 0$ decays to zero exponentially fast [$\text{Re}(\eta) \geq 0$ is required for stability]. In this case, the monitored long-range hopping dynamics are effectively reduced to a nearest neighbor hopping model. This short-ranged model undergoes a Berezinskii-Kosterlitz-Thouless (BKT) transition from a critical to an area law phase as a function of the measurement strength. This scenario is discussed in detail in Refs. [13,14]. (b) For $p \leq 3/2$, the long-range hopping is relevant and strongly enhances fluctuations of ϕ_x. This can be seen already on the level of first order RG equations: any $|\Delta| > 0$ enforces a rapid decrease of η in Eq. (8) [59]. This confirms the result from canonical power counting. (c) Although Eq. (7) is reminiscent of a conventional sine-Gordon model (here for a p-dependent canonical scaling dimension), the transition between the critical and the long-range phase does not match the BKT paradigm. The reason is the linear appearance of Δ in Eq. (8), obtained at first order perturbation theory. It gives rise to an unconventional transition, which is characteristic for long-range coupled systems [32]. (d) A similar argument applies for the transition from the area law to the long-range phase. This transition arises from the direct competition between the two cosine terms. For a short-ranged sine-Gordon model, this gives rise to a sequence of universality classes depending on the factor in the nonlinearities, including the Ising and parafermionic ones [60]. However, due to Eq. (8), this is again different for the long-range model, where a transition of this type has not yet been characterized.

Characterizing the algebraic scaling phase.—For $p \leq 3/2$, the long-range hopping, and the coupling Δ, are relevant. The dark state $|\psi_D\rangle$, as well as the fermion entanglement entropy and correlation functions, are then modified by the impact of $\hat{H}_{\text{lr}}$ in Eq. (4). It pushes the phases $\hat{\theta}_l$ of the fermion operators $\hat{c}_l, \hat{c}_l^\dagger$ to align with each other, and to pin the argument of $\cos\sqrt{2}(\hat{\theta}_x - \hat{\theta}_y)$ at small values. Expanding $\hat{H}_{\text{eff}}$ up to second order in $\hat{\theta}_x$ yields (in Fourier space)

$$\hat{H}_{\text{eff}} = \int_q q^2\{-i\Delta_p|q|^{2p-3}\hat{\theta}_{-q}\hat{\theta}_q + \eta\hat{\phi}_{-q}\hat{\phi}_q\}, \qquad (9)$$

with a positive integration constant Δ_p (see Ref. [52]). The terms $\sim\hat{\theta}_q$ in $\hat{H}_{\text{eff}}$ become more and more dominant as $q \to 0$. This governs the dark state $|\psi_D\rangle$ at long wavelength

(see Ref. [52]), such that the correlation functions and the entanglement entropy acquire a p-dependent scaling exponent [61],

$$S(l) \sim B|l|^b + s_0, \qquad b = \frac{3}{2} - p, \qquad (10)$$

$$C(l) \sim A|l|^{-a}, \qquad a = p + \frac{1}{2}. \qquad (11)$$

This analytical estimate is confirmed by the numerical simulations very accurately, which is demonstrated in Figs. 1(d),1(e) Fig. 2 (purple lines), and Ref. [52]. These scaling exponents clearly differ from the volume law $b = 1$, found, for instance, in monitored random circuits [4,51,62–67]. We find a slower growth of the entanglement entropy $b < 1/2$, matching the scaling relation $b = 2 - a$ [see Fig. 3(b)], implied by Eq. (6).

Conclusion.—Long-range dynamics leads to a novel measurement-induced subvolume phase with a maximum entanglement growth exponent $S \sim \sqrt{L}$. Despite the enhanced entangling effect of long range hoppings, the system does not reach a volume law characteristic of an ergodic phase. Indeed, a volume law is typically associated with excited or generic states, located in the middle of the spectrum of a Hamiltonian. Here, the trajectory wave functions evolve to states that bear strong similarities to ground states. In fact, it is intriguing to notice the similarity of the phase structure to the ground state phase diagram of long-range interacting spin models in one dimension [32], where the density pinning effect of measurements is replaced by nearest neighbor interactions. This suggests a persistence of quantum ground state dynamics in the trajectory wave function, which is reflected in the effective *cooling* towards measurement-induced dark states in the replica formalism. It will be exciting to identify the precise criteria for the breakdown of the scenario reported here, the occurrence of true volume law phases or classical vs quantum phase transitions in trajectory ensembles, e.g., in terms of the Gaussianity of the state present here, or of the integrability of the generator of dynamics [68–70]. The existence of a MIPT from an entangling to a disentangling phase was observed recently in an experimental quantum circuit [71]. Extending this setup in order to resolve the entanglement scaling with distance, i.e., by introducing spatially separated auxiliary qubits, could be a promising step towards distinguishing different entangling phases.

Note added.—Recently, we became aware of two complementary works on the MIPT in long-range coupled Hamiltonian systems [73,74], where a critical hopping exponent p_c relatable to our $p_c = 3/2$ was identified.

[1] B. Skinner, J. Ruhman, and A. Nahum, Phys. Rev. X **9**, 031009 (2019).

[2] Y. Li, X. Chen, and M. P. A. Fisher, Phys. Rev. B **98**, 205136 (2018).

[3] Y. Li, X. Chen, and M. P. A. Fisher, Phys. Rev. B **100**, 134306 (2019).

[4] M. J. Gullans and D. A. Huse, Phys. Rev. X **10**, 041020 (2020).

[5] S. Choi, Y. Bao, X.-L. Qi, and E. Altman, Phys. Rev. Lett. **125**, 030505 (2020).

[6] C.-M. Jian, Y.-Z. You, R. Vasseur, and A. W. W. Ludwig, Phys. Rev. B **101**, 104302 (2020).

[7] R. Fan, S. Vijay, A. Vishwanath, and Y.-Z. You, Phys. Rev. B **103**, 174309 (2021).

[8] Y. Li and M. P. A. Fisher, Phys. Rev. B **103**, 104306 (2021).

[9] A. Nahum, S. Roy, B. Skinner, and J. Ruhman, PRX Quantum **2**, 010352 (2021).

[10] Y. Fuji and Y. Ashida, Phys. Rev. B **102**, 054302 (2020).

[11] S.-K. Jian, C. Liu, X. Chen, B. Swingle, and P. Zhang, Phys. Rev. Lett. **127**, 140601 (2021).

[12] E. V. H. Doggen, Y. Gefen, I. V. Gornyi, A. D. Mirlin, and D. G. Polyakov, arXiv:2104.10451.

[13] O. Alberton, M. Buchhold, and S. Diehl, Phys. Rev. Lett. **126**, 170602 (2021).

[14] M. Buchhold, Y. Minoguchi, A. Altland, and S. Diehl, Phys. Rev. X **11**, 041004 (2021).

[15] Y. Bao, S. Choi, and E. Altman, Ann. Phys. (Amsterdam) 168618 (2021).

[16] X. Turkeshi, A. Biella, R. Fazio, M. Dalmonte, and M. Schiró, Phys. Rev. B **103**, 224210 (2021).

[17] M. Ippoliti, M. J. Gullans, S. Gopalakrishnan, D. A. Huse, and V. Khemani, Phys. Rev. X **11**, 011030 (2021).

[18] Y. Ashida, S. Furukawa, and M. Ueda, Phys. Rev. A **94**, 053615 (2016).

[19] Y. Ashida, S. Furukawa, and M. Ueda, Nat. Commun. **8**, 15791 (2017).

[20] G. Mazzucchi, S. F. Caballero-Benitez, D. A. Ivanov, and I. B. Mekhov, Optica **3**, 1213 (2016).

[21] G. Mazzucchi, W. Kozlowski, S. F. Caballero-Benitez, T. J. Elliott, and I. B. Mekhov, Phys. Rev. A **93**, 023632 (2016).

[22] S. Dhar and S. Dasgupta, Phys. Rev. A **93**, 050103(R) (2016).

[23] D. A. Ivanov, T. Y. Ivanova, S. F. Caballero-Benitez, and I. B. Mekhov, Phys. Rev. Lett. **124**, 010603 (2020).

[24] G. Buonaiuto, F. Carollo, B. Olmos, and I. Lesanovsky, Phys. Rev. Lett. **127**, 133601 (2021).

[25] Y. Minoguchi, P. Rabl, and M. Buchhold, arXiv:2108.04256.

[26] S. Wolff, J.-S. Bernier, D. Poletti, A. Sheikhan, and C. Kollath, Phys. Rev. B **100**, 165144 (2019).

[27] S. Wolff, A. Sheikhan, and C. Kollath, SciPost Phys. Core **3**, 010 (2020).

[28] D. Poletti, J.-S. Bernier, A. Georges, and C. Kollath, Phys. Rev. Lett. **109**, 045302 (2012).

[29] H. Pichler, A. J. Daley, and P. Zoller, Phys. Rev. A **82**, 063605 (2010).

[30] A. Campa, T. Dauxois, D. Fanelli, and S. Ruffo, *Physics of Long-Range Interacting Systems* (Oxford University Press, New York, 2014).

[31] A. Dutta and J. K. Bhattacharjee, Phys. Rev. B **64**, 184106 (2001).

[32] M. F. Maghrebi, Z.-X. Gong, and A. V. Gorshkov, Phys. Rev. Lett. **119**, 023001 (2017).

[33] P. Hauke and L. Tagliacozzo, Phys. Rev. Lett. **111**, 207202 (2013).

[34] J. Schachenmayer, B. P. Lanyon, C. F. Roos, and A. J. Daley, Phys. Rev. X **3**, 031015 (2013).

[35] P. Richerme, Z.-X. Gong, A. Lee, C. Senko, J. Smith, M. Foss-Feig, S. Michalakis, A. V. Gorshkov, and C. Monroe, Nature (London) **511**, 198 (2014).

[36] J. W. Britton, B. C. Sawyer, A. C. Keith, C.-C. J. Wang, J. K. Freericks, H. Uys, M. J. Biercuk, and J. J. Bollinger, Nature (London) **484**, 489 (2012).

[37] P. Jurcevic, B. P. Lanyon, P. Hauke, C. Hempel, P. Zoller, R. Blatt, and C. F. Roos, Nature (London) **511**, 202 (2014).

[38] J. Zhang, G. Pagano, P. W. Hess, A. Kyprianidis, P. Becker, H. Kaplan, A. V. Gorshkov, Z.-X. Gong, and C. Monroe, Nature (London) **551**, 601 (2017).

[39] R. Landig, L. Hruby, N. Dogra, M. Landini, R. Mottl, T. Donner, and T. Esslinger, Nature (London) **532**, 476 (2016).

[40] F. Mivehvar, F. Piazza, T. Donner, and H. Ritsch, Adv. Phys. **70**, 1 (2021).

[41] P. Schauß, M. Cheneau, M. Endres, T. Fukuhara, S. Hild, A. Omran, T. Pohl, C. Gross, S. Kuhr, and I. Bloch, Nature (London) **491**, 87 (2012).

[42] B. Yan, S. A. Moses, B. Gadway, J. P. Covey, K. R. A. Hazzard, A. M. Rey, D. S. Jin, and J. Ye, Nature (London) **501**, 521 (2013).

[43] The numerical results match the analytical predictions with very high accuracy and we use the analytical identities for a, b, p_c here and in the following.

[44] M. Ippoliti, T. Rakovszky, and V. Khemani, arXiv:2103.06873.

[45] X. Cao, A. Tilloy, and A. D. Luca, SciPost Phys. **7**, 24 (2019).

[46] N. Gisin and I. C. Percival, J. Phys. A **25**, 5677 (1992).

[47] H. M. Wiseman and G. J. Milburn, Phys. Rev. A **47**, 1652 (1993).

[48] M. Szyniszewski, A. Romito, and H. Schomerus, Phys. Rev. B **100**, 064204 (2019).

[49] D. Yang, C. Laflamme, D. V. Vasilyev, M. A. Baranov, and P. Zoller, Phys. Rev. Lett. **120**, 133601 (2018).

[50] A. Nahum, J. Ruhman, S. Vijay, and J. Haah, Phys. Rev. X **7**, 031016 (2017).

[51] Y. Bao, S. Choi, and E. Altman, Phys. Rev. B **101**, 104301 (2020).

[52] See Supplemental Material at http://link.aps.org/supplemental/10.1103/PhysRevLett.128.010605 for a derivation of the long-range replica Hamiltonian and the perturbative RG equations, a discussion of observables in bosonization, and further details on the numerical study, which includes Refs. [11,13–15,53–56].

[53] L. M. Sieberer, M. Buchhold, and S. Diehl, Rep. Prog. Phys. **79**, 096001 (2016).

[54] P. Calabrese and J. Cardy, J. Phys. A **42**, 504005 (2009).

[55] H. Casini and M. Huerta, J. Phys. A **42**, 504007 (2009).

[56] P. Calabrese and J. Cardy, J. Stat. Mech. (2004) P06002.

[57] P. Zhang, S.-K. Jian, C. Liu, and X. Chen, arXiv:2104.04088.

[58] Two spatial integrals, one temporal integral and the factor $|y|^{-2p}$, i.e., $dt\, dx\, dy y^{-2p}$ scale like b^{3-2p} with a distance b.

[59] For a conventional sine-Gordon model with short-range nonlinearity, the renormalization of η starts at the level of second order perturbation theory.

[60] P. Lecheminant, A. O. Gogolin, and A. A. Nersesyan, Nucl. Phys. **B639**, 502 (2002).

[61] Variable, measurement-induced exponents have also been reported in the time domain in Ref. [23].

[62] A. Zabalo, M. J. Gullans, J. H. Wilson, S. Gopalakrishnan, D. A. Huse, and J. H. Pixley, Phys. Rev. B **101**, 060301(R) (2020).

[63] L. Zhang, J. A. Reyes, S. Kourtis, C. Chamon, E. R. Mucciolo, and A. E. Ruckenstein, Phys. Rev. B **101**, 235104 (2020).

[64] Q. Tang and W. Zhu, Phys. Rev. Research **2**, 013022 (2020).

[65] X. Chen, Y. Li, M. P. A. Fisher, and A. Lucas, Phys. Rev. Research **2**, 033017 (2020).

[66] M. J. Gullans and D. A. Huse, Phys. Rev. Lett. **125**, 070606 (2020).

[67] A. Nahum and B. Skinner, Phys. Rev. Research **2**, 023288 (2020).

[68] A. A. Ziolkowska and F. H. Essler, SciPost Phys. **8**, 44 (2020).

[69] F. H. L. Essler and L. Piroli, Phys. Rev. E **102**, 062210 (2020).

[70] O. Lunt and A. Pal, Phys. Rev. Research **2**, 043072 (2020).

[71] C. Noel, P. Niroula, D. Zhu, A. Risinger, L. Egan, D. Biswas, M. Cetina, A. V. Gorshkov, M. J. Gullans, D. A. Huse, and C. Monroe, arXiv:2106.05881.

[72] J. Bezanson, A. Edelman, S. Karpinski, and V. B. Shah, SIAM Rev. **59**, 65 (2017).

[73] T. Minato, K. Sugimoto, T. Kuwahara, and K. Saito, this issue, Phys. Rev. Lett. **128**, 010603 (2022).

[74] M. Block, Y. Bao, S. Choi, E. Altman, and N. Y. Yao, preceding Letter, Phys. Rev. Lett. **128**, 010604 (2022).